Pendulum Impact Tests of Wooden and Steel Highway Guardrail Posts

by Charles J. Gatchell
and Jarvis D. Michie

USDA FOREST SERVICE RESEARCH PAPER NE-311
1974

NORTHEASTERN FOREST EXPERIMENT STATION
FOREST SERVICE, U.S. DEPARTMENT OF AGRICULTURE
6816 MARKET STREET, UPPER DARBY, PA. 19082
F. BRYAN CLARK, STATION DIRECTOR

The Authors

CHARLES J. GATCHELL received his B.S. degree in forestry from the University of Massachusetts in 1955. After serving a tour of duty as an air intelligence officer with the U. S. Navy, he attended the New York State University College of Forestry at Syracuse University where in 1961 he received his M.S. degree in wood-products engineering. From 1961 to 1965 he was a project scientist in the product- and process-development project at the Forest Products Laboratory in Madison, Wisconsin. He is now project leader of the hardwood-product improvement work unit at the Forest Products Marketing Laboratory of the Northeastern Forest Experiment Station in Princeton, West Virginia.

JARVIS D. MICHIE received a B.S. degree in civil engineering from the University of Texas (Austin) in 1955 and an M.S. degree in structural engineering from Louisiana State University in 1961. He has been associated with the Southwest Research Institute, San Antonio, Texas, since 1963 and is presently manager of its Transportation Structural Systems Section. Since 1967 he has been active in highway and vehicle safety research, with particular emphasis on traffic-barrier technology.

MANUSCRIPT RECEIVED FOR PUBLICATION 30 MAY 1974

ABSTRACT

Impact strength characteristics of southern pine, red oak, and steel highway guardrail posts were evaluated in destructive impact testing with a 4,000-pound pendulum at the Southwest Research Institute. Effects were recorded with high-speed motion-picture equipment. Comparisons were based on reactions to the point of major post failure. Major comparisons of 6x6-inch and 6x8-inch red oak and southern pine posts with W6x8.5 and S3x5.7 steel posts showed wooden posts to be equal or superior to steel. The basis for wooden-post specifications should be the amount of knot-associated grain distortion in the middle third of the tension face of the posts. Acceptable posts are those with no single knot in the middle third of the tension face that disorients the grain for more than one-third the width of the face.

Pendulum Impact Tests of Wooden and Steel Highway Guardrail Posts

Contents

GUARDRAIL POSTS

GUARDRAILS are important for protecting people on our highways. The design of a guardrail system—in which variables such as vehicle speed, weight, and angle of approach must be considered—represents a compromise of service requirements.

The relatively few full-scale crash tests made usually involve a 4,000-pound vehicle that is crashed into a barrier at an approach angle of 25 degrees and a speed of 60 miles per hour. Such a test costs several thousand dollars. Experience has shown that test results under one set of conditions should not be applied to other greatly different sets of conditions.

In the widely used semi-rigid strong-post guardrail system, the energy of a vehicle hitting it is transmitted to the earth by the posts supporting the flex or W-beam rail. Because the posts are the key to successful performance of a guardrail system, evaluating them without the high cost of full-scale crash-testing poses a challenge to researchers.

After a preliminary investigation (*Michie et al 1971*) the Forest Products Marketing Laboratory contracted with the Southwest Research Institute of San Antonio, Texas, to evaluate the dynamic performance of wooden and steel guardrail posts, using the technique of pendulum testing. A major objective was to determine if posts smaller in cross-section than the standard 8x8-inch wooden post would compare favorably with the W6x8.5 steel post. We found that 6x8 southern pine posts and 6x6 red oak posts showed generally superior characteristics.

TESTING FACILITY

Pendulum

The Southwest Research Institute testing facility consisted of a pendulum, operating equipment, test-control and data-acquisition instrumentation, and high-speed motion-picture equipment (fig. 1). A 4,000-pound pendulum with an accelerometer mounted at the rear was suspended on a 26-foot swing radius in such a manner that it remained horizontal throughout the swing arc.

The posts were fixed at the lowest point of the pendulum arc, where the kinetic energy of

Figure 1.—The pendulum test facility.

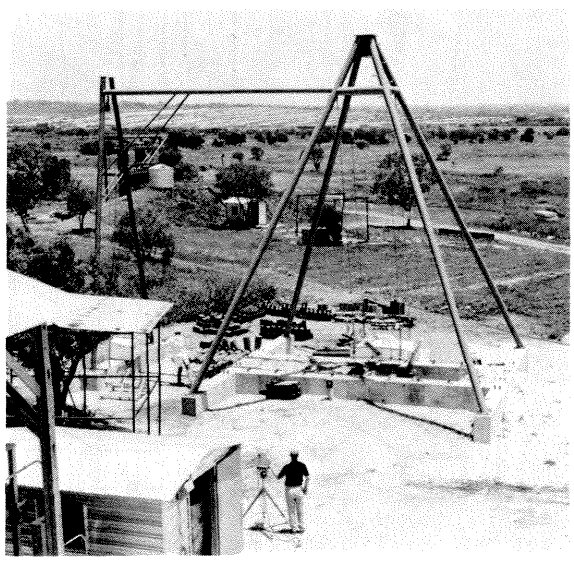

the mass was greatest. For these tests, the impact velocity was slightly less than 20 miles per hour. This combination of mass and speed approximates the normal force component of a 4,000-pound vehicle hitting a guardrail at a speed of 60 miles per hour and an angle of 25 degrees.

The pendulum mass was a 3x6x1.5-foot block of reinforced concrete to the front face of which was attached an 8-inch diameter extra-heavy steel pipe filled with concrete for making contact with the post. A 1-inch thick pad of 70 durometer neoprene was attached to the surface of the steel bumper.

Post Holder

Because our objective was to evaluate the post rather than soil characteristics, the post holder (fig. 2) was designed to simulate frozen ground.

The front of the holder was an ⌶-shaped member made of two 5-foot lengths of 6x8 steel box beam welded to a 1½-foot center section of 6x8 box beam. The ends of the 5-foot members were bolted to the concrete walls of the pendulum facility foundation.

The back of the post holder was a T made of 6x8 box beam. The crossbar top, welded to the upright, was positioned so its 6-inch face was across the 8-inch face of the upright (fig. 2). A slope was cut on the upper front face of the upright to prevent a sharp edge from affecting the reaction of the wooden posts to impact. A 2-inch pad of polyurethane was attached to the front of the crossbar.

For testing steel posts, the holder was modified to assure structural failure of the post above the clamp. The slope on the front face of the T was filled with a wooden block, and a metal brace was substituted for the polyurethane pad to minimize twisting of the steel post and to develop the maximum resistance about the strong axis of the post.

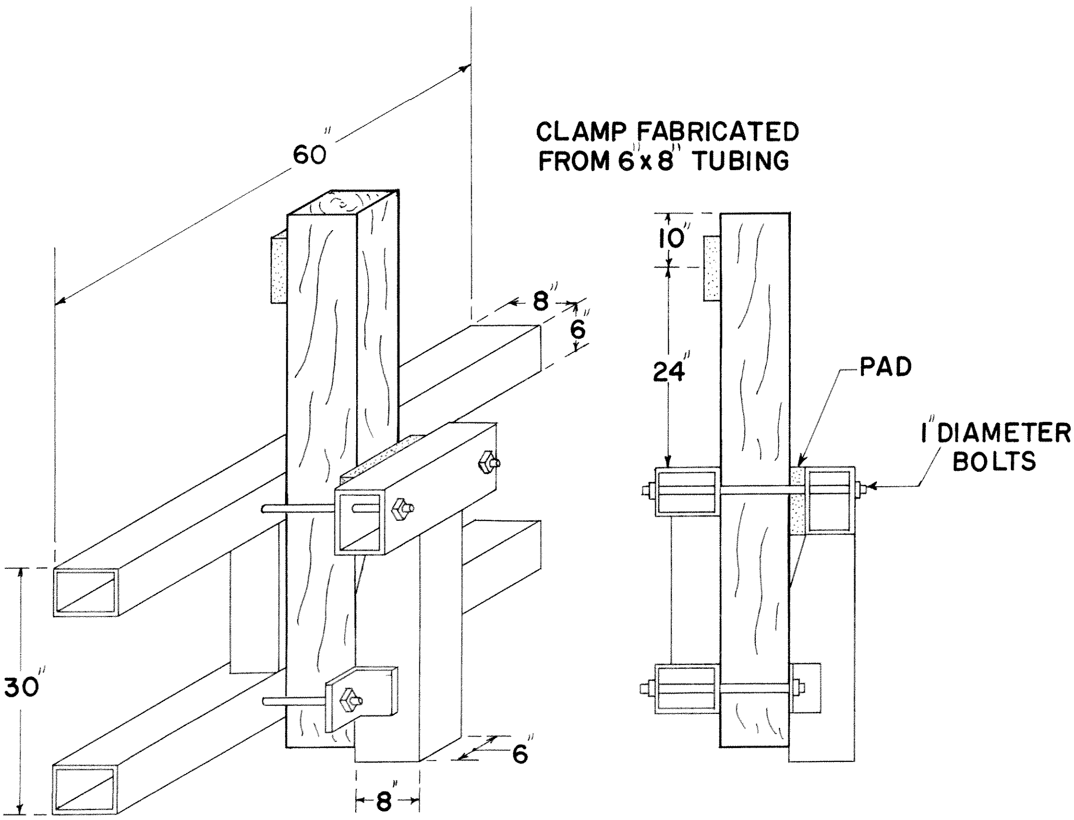

Figure 2.—Construction details of the post holder.

Preparation of Posts for Testing

To make identification of post failures easier, the top half of the front face of each wooden post was painted white. A 1-inch thick attenuation pad of 70 durometer neoprene was attached to each wooden post at the point of pendulum contact. An 8x8x12-inch wooden block was bolted to the front face of each steel post to act as an initial force attenuator and to insure overbending of the steel post so that it would not interfere with the pendulum mass on the backswing.

THE POSTS

Eight series of posts were tested:

Series	*Description*
RO 66	6x6-inch sound-square-edge boxed-heart red oak.
RO 68	6x8-inch sound-square-edge boxed-heart red oak.
SP 66	6x6-inch No. 1 SR boxed-heart southern yellow pine.
SP 68	6x8-inch No. 1 SR boxed-heart southern yellow pine.
SP 68_c	6x8-inch No. 1 dense SR boxed-heart creosote-treated southern yellow pine.
SP 86	6x8-inch No. 1 SR boxed-heart southern yellow pine (loading about the minor axis).
S3x5.7	S3x5.7 steel posts (standard AISC shape).
W6x8.5	W6x8.5 steel posts (standard AISC shape).

The steel posts were supplied by Southwest Research Institute from its own inventory. The red oak posts were purchased on the open market by the Forest Products Marketing Laboratory. The southern pine posts were contributed through the cooperation of the Southern Forest Products Association and Colfax Creosoting Company of Pineville, Louisiana.

All wooden posts were boxed-heart. Except for the creosote-treated southern pine pieces, all wooden posts were selected for evaluating potentially important characteristics. For example, in the untreated SP 68 series, posts A, B, and C had the pith centered and no knots in the middle third of each post; posts D and E had large knots in the center zone, and the pith was located just below the tension or compression face; post F had no knots in the middle third, but the pith was located near the surface of the piece; and post G had a centered pith and knots in the middle third. As far as possible, this pattern was followed with all other southern pine series.

Selection of red oak posts was limited to posts with or without knots in the central portion.

DATA GENERATION

Signals from an accelerometer, mounted at the rear of the pendulum mass, were continuously recorded throughout impact by a high-speed tape recorder operating at a speed of 60 inches per second. The tape was then played through an oscillograph, and tracings were recorded. Using Newton's second law of motion:

$$F = ma$$

the post resisting force (F) was determined from the pendulum mass (m) and its instantaneous deceleration (a). By applying the proper scales for force and time, the oscillograph tracings were converted to force-time curves.

The pendulum impact or initial velocity (V_o) was determined with signals from a crack-wire speed-trap. The peak resistance force and time of resistance to impact could be taken directly from the force-time curves. Other important parameters were calculated. These were:

1. Final pendulum velocity—(V_f).

   The area under the force-time curve is linear impulse and is expressed by

$$\int_{t_o}^{t_f} Fdt = m\,(V_f - V_o)$$

   where F is the resistance force acting on the pendulum mass, m is the pendulum mass, and V_o and V_f are the initial and final velocities. The impulse was measured by a planimeter, and the final velocity was calculated by

$$V_f = V_o - \frac{\text{Linear Impulse}}{m}$$

2. Fracture energy—(FE).
   The fracture energy is the change in kinetic energy resulting from impact. It was obtained from

$$FE = \frac{1}{2} m (V_f^2 - V_o^2)$$

3. Post displacement during impact—(d).
   The pendulum mass velocity was assumed to change linearly with time. Thus, the displacement of the post during contact with the pendulum was determined from

$$d = \left(\frac{V_f + V_o}{2}\right) (t_f - t_o)$$

4. Average force during post displacement—(F_{avg}).
   The average force is an idealized constant force that acts through the distance of post displacement during impact. It was derived from dividing the fracture energy by the post displacement. Thus

$$F_{avg} = \frac{FE}{d}$$

METHOD OF ANALYSIS

The pendulum-impact test can be viewed in two ways. The first approach simulates a head-on crash of a 4,000-pound vehicle traveling at a speed of almost 20 miles per hour and hitting a single post in frozen ground. The total impulse and total time of post resistance are used in calculating the various post parameters. Results based on the total effects are available from the Northeastern Forest Experiment Station, Forest Products Marketing Laboratory, Princeton, West Virginia 24740.

In the second approach, used in this report, we considered the same test conditions to represent the normal force of a 4,000-pound vehicle hitting a barrier at a speed of 60 miles per hour and an approach angle of about 25 degrees. These conditions are normally used in full-scale crash tests of barrier systems.

In systems using strong wooden posts and steel-beam guardrail, wooden posts are rarely broken, and the energy is absorbed during deformation of the vehicle and soil. If a wooden post breaks, the tension in the rail transmits the impact to adjacent posts. During initial stages of impact, eight or more posts may be transmitting the load to the ground. For comparing post sizes and materials where a guardrail is used, analysis of force-time curves to the point of major failure is more precise than considerations of total effects.

Beyond the point of major failure, it is difficult to compare wooden and steel posts, because wooden posts suffer a major material failure whereas steel posts suffer a major structural failure. Once the steel post fails initially, the subsequent displayed force is largely that used to bend the post around the top of the post holder.

The time of force generation is a factor in calculating such parameters as final pendulum velocity, fracture energy, and post displacement. Post displacement is used to calculate the average force acting on the post during impact. Once the major failure occurs, the rate of displacement of the post top increases. By terminating the analysis at the point of major failure, the precision of comparisons is increased.

The point of major failure can be pinpointed clearly by analysis of the high-speed motion-picture film in conjunction with the force-time curves. The movies were taken at either 580 or 880 frames per second. When the pendulum was swinging from left to right, the clamp could be observed on the film to move slightly downward and to the right. It remained in this position until visible failure occurred in the post, and/or a sharp decrease in the force-time curves was noted. Then it returned to its original position. By knowing the speed of the film and by counting the individual frames, we could locate the point of major failure on the force-time curves with no greater than 1 msec (millisecond) error for the slower speed film (580 frames per second) and 0.5 msec error for the higher speed film (880 frames per second).

In bending, wood is subjected to three types of basic stress: tension, compression, and shear. In a guardrail post, the face receiving the impact is in tension and the opposite face is in compression (fig. 3). Where shear is

Figure 3. — Location of stresses during impact.

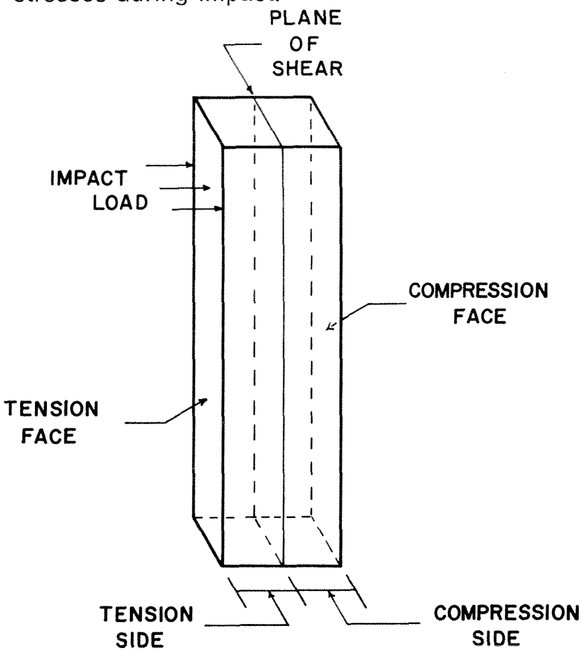

likely (as with oak), it will generally occur in a plane parallel to the tension face and at or near the center of the post.

Since posts usually are inserted in the ground to a depth equal to about half their length, the greatest forces can be expected to occur in the middle third of the post. When the ground is frozen, the post acts as a cantilever beam, and the major stress will occur at the ground line or middle of the post. When the ground is very soft, the post is free to pivot and post properties are not significant.

In between these extremes are found the conditions of "normal" use. The top of the post moves in the direction of the applied force. As the post moves, the soil at the ground line is compressed and offers increased resistance to the middle third of the post. If we assume adequate resistance of the soil, the bottom of the post is essentially restrained from movement and the maximum tensile stresses will occur in the middle third of the post.

Examples of force-time curves and failure sequences are given in figures 4, 5, and 6. The first force peak in each wooden post curve represents an acceleration of the post to the speed of the pendulum. It is unlikely that any damage to the wooden post occurs here. Once the post and pendulum are moving at the same speed, the accelerometer on the pendulum records no resistance, and the force curve falls toward zero.

As the wooden post bends, it stiffens; and the second peak occurs. During this period, the clamp is moving downward and to the right. At about the time of peak resistance, a major failure occurs in the wooden post. The curve then drops abruptly to zero. Examination of the broken posts in conjunction with force-time curve and high-speed motion-picture film analysis provided an evaluation of strength-reducing defects.

RESULTS

General

In these dynamic tests, the shape of the force-time curve is a result of impact velocity. As long as the tests are dynamic, the impulse or area under the curve should remain the same. At lower impact speeds, we would expect smaller peak forces and longer periods of resistance, the fracture energy remaining about the same. Rather than being absolute, the force-time curves and calculated impact values should be considered indexes of behavior that are useful for making comparisons.

The strength properties of a wooden post depend primarily upon density and location of defects, especially knots. Within a species, speed of application of load and location of defects are of great importance. Dynamic loading can produce strength values that are two or three times those of static tests. It is the dynamic values from impact loads that we are concerned with when discussing guardrail posts.

Almost all the strength properties of wood increase significantly as wood dries below the fiber saturation point of about 30 percent moisture content. However, in posts of guardrail size, this normal increase in strength may not occur because of the development of checks around knots and in the area near the shear plane. Drying checks have little, if any, effect on strength in tension, and only a slight negative effect on strength in compression.

In sound posts, knots are the single most

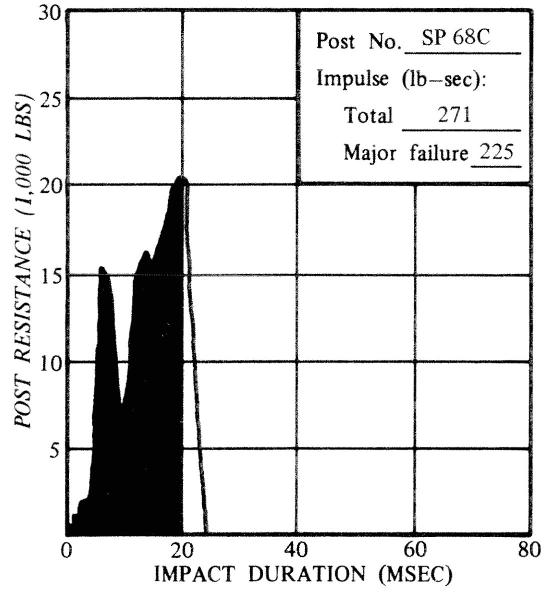

Figure 4.—Force-time curve and failure sequence for southern pine post SP 68C (1 msec = 0.001 second).

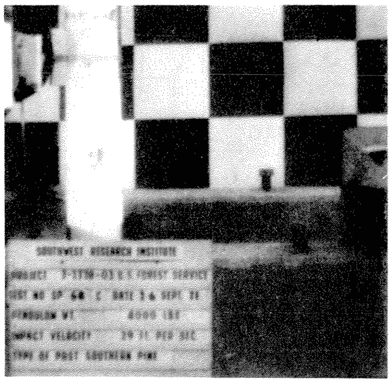

T = 0 msec

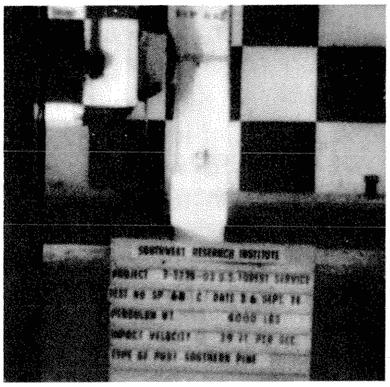

T = 6 msec

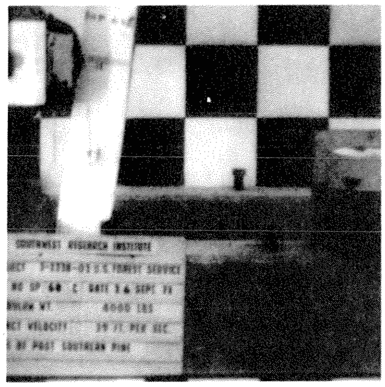

T = 15 msec

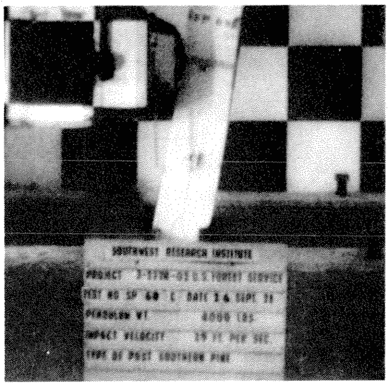

T = 16 msec

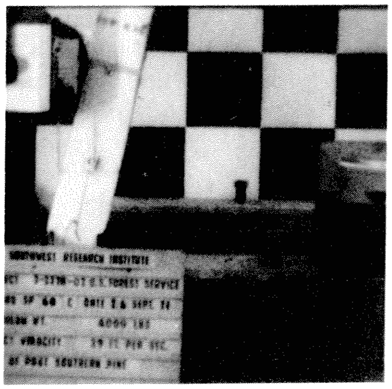

T = 17 msec

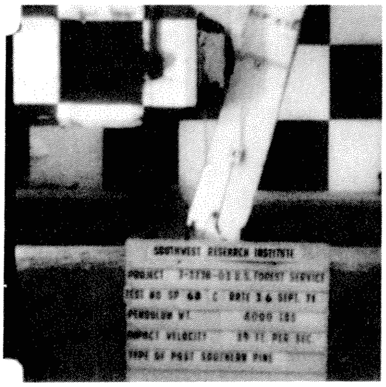

T = 19 msec

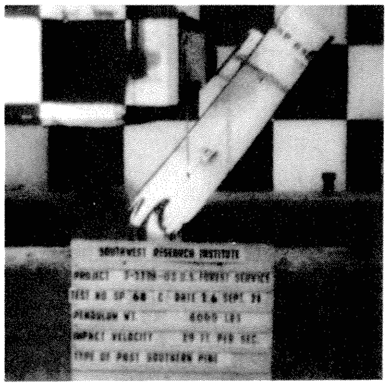

T = 28 msec

At T = 0 msec, the pendulum contacts the attenuation pad. At T = 6 msec, the pendulum has compressed the pad and has met with post resistance, thus forming the first peak in the forcetime curve. The pendulum and the post move at the same velocity and, as there is no post resistance, the curve drops down. At T = 15 msec, the post is offering resistance, but there is no visible damage. At T = 16 msec, failure at the clamp on the tension side begins and continues across the cross-section through T = 17 msec until complete at T = 19 msec. At T = 28 msec, failure is clearly shown and, from the point of major failure at T = 19 msec, the post top has sprung ahead of the pendulum.

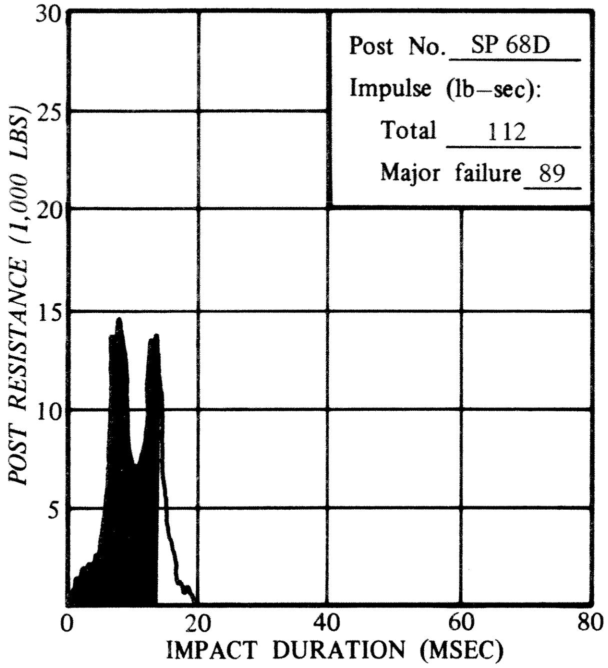

Figure 5.—SP 68D force-time curve and failure sequence for southern pine post SP 68D (1 msec = 0.001 second).

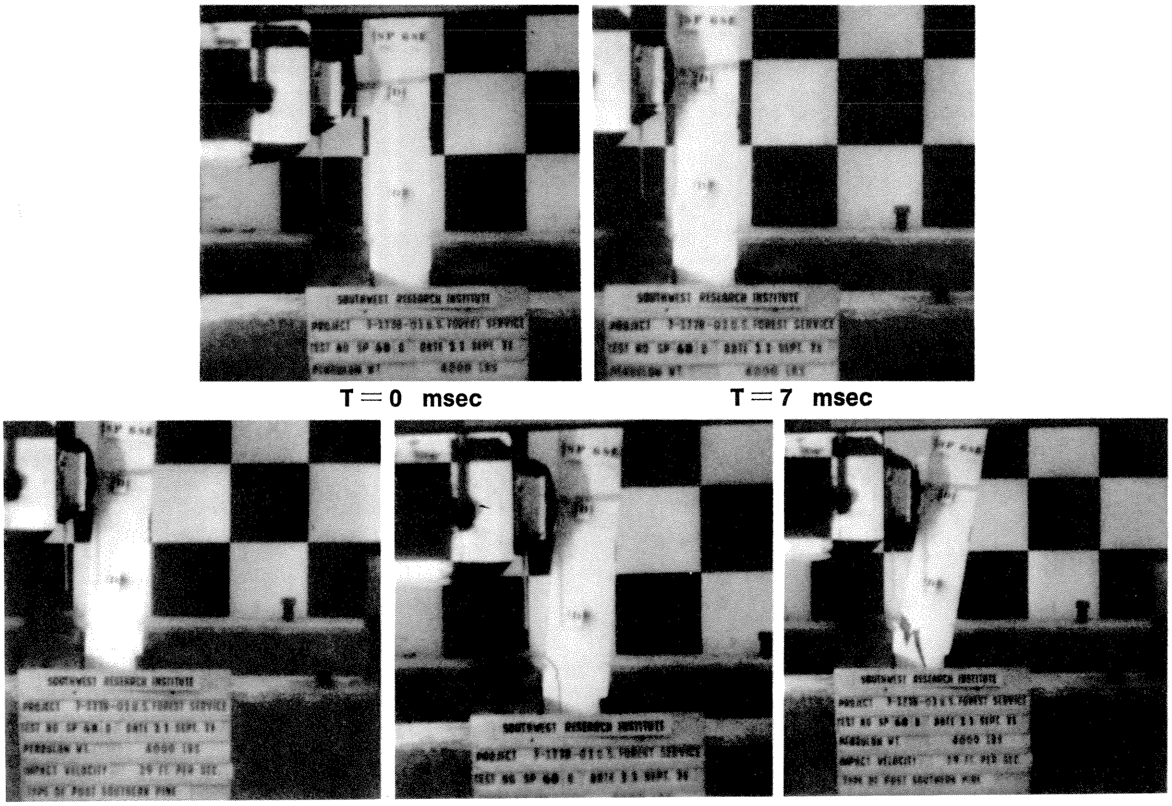

T = 0 msec **T = 7 msec**

T = 12 msec **T = 14 msec** **T = 19 msec**

As in figure 3, T = 0 msec and T = 7 msec show the compression of the attenuation pad and the generation of the first peak force. At T = 12 msec, the post is again offering resistance. At T = 14 msec, drastic post failure begins, owing to severe knot-caused grain distortion on the tension face. By T = 15 msec, the major failure, as clearly shown at T = 19 msec, is about complete.

Figure 6.—Force-time curve and failure sequence for southern pine post SP 68F (1 msec = 0.001 second).

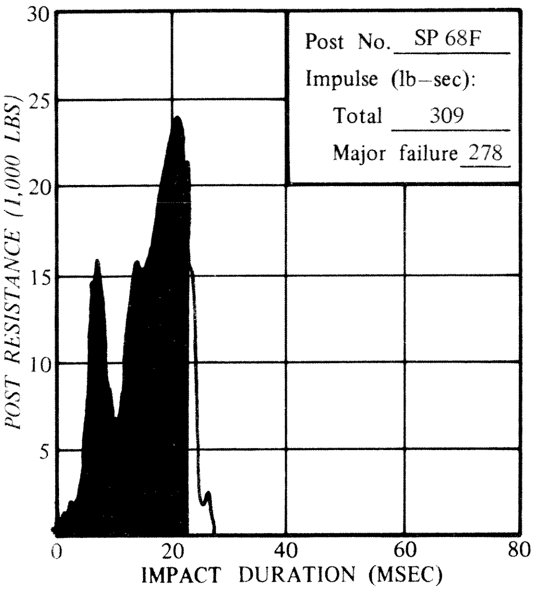

T = 0 msec

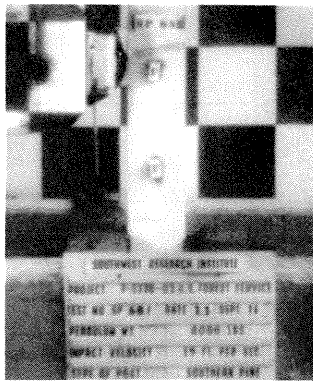

T = 6 msec

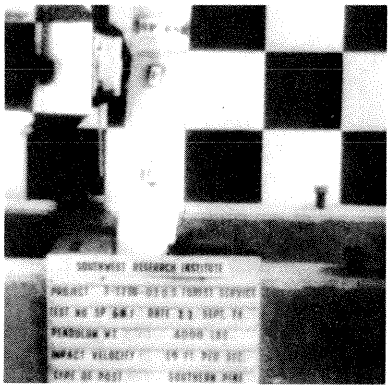

T = 9 msec

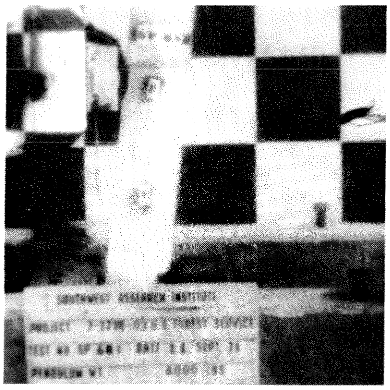

T = 14 msec

T = 16 msec

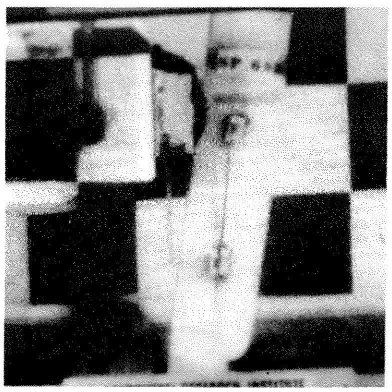

T = 17 msec

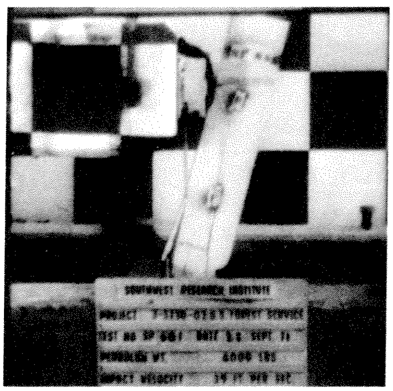

T = 20 msec

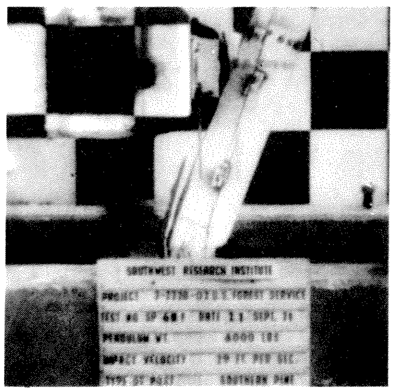

T = 24 msec

As in figure 3, T = 0 msec and T = 6 msec show the compression of the attenuation pad and the generation of the initial peak force. At T = 9, 14, and 16 msec, the post is bent, with no visible damage. At T = 17 msec, failure begins as a crack appears on the front face between the two letter "F's". At T = 20 msec, major failure on the tension face and across the cross-section is visible. Also, shear has occurred. At T = 24 msec there is no post resistance and shear is apparent.

Figure 7.—Examples of knot influence on post reaction to impact. Note: all failures occurred in the middle third of the post.

Non-Critical Knots

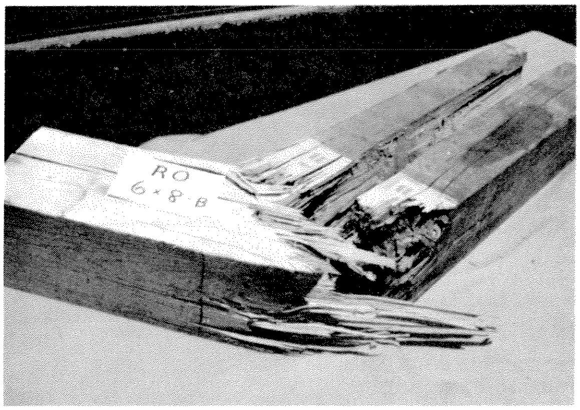

RO 68B. A 2-inch knot on corner of front and tension faces was located 2 inches below the clamp. Grain distortion extended across one-fourth the width of the tension face. Post impact strength: above average for the RO 68 series.

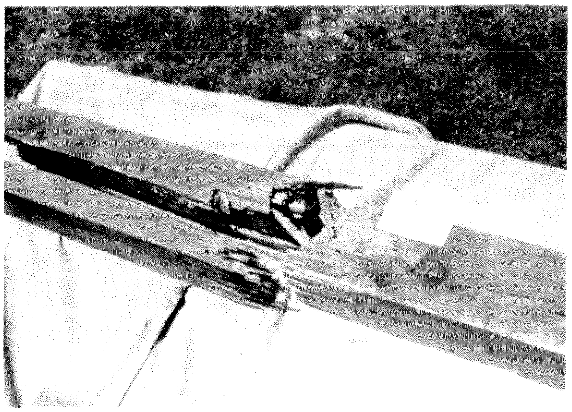

RO 68G. Two small knots (½ and 1 inch) in the middle of the back face were located 2 inches above the clamp. Post impact strength: above average for the RO 68 series.

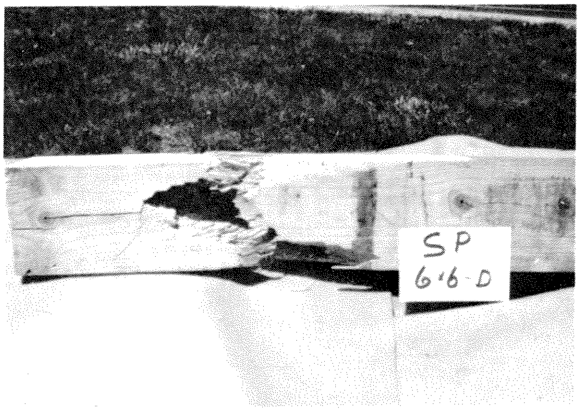

SP 66D. Failure occurred at the clamp midway between knots clusters on the tension face. No single knot disoriented the grain for more than one-third the width of the tension face. Post impact strength: average for the SP 66 series.

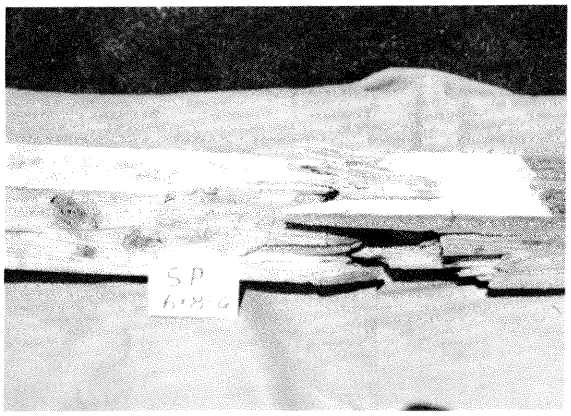

SP 68G. Three knots were located 4 to 6 inches above the clamp on the tension face. No knot disoriented the grain for more than one-third the width of the tension face. Post impact strength: above average for the SP 68 series.

Critical Knots

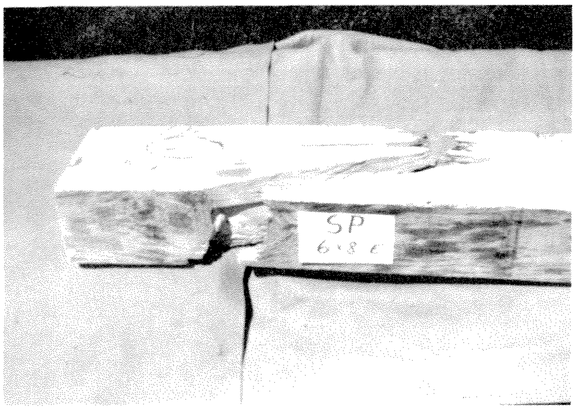

SP 68E (two views, above): a 1½-inch knot located about 11 inches above the clamp on the tension face disoriented the grain across the entire 6-inch width of the face. Other knots from the same cluster on front and compression faces had no effect on strength. Post impact strength: far below average for the SP 68 series.

RO 68E (two views, below): a 3-inch knot located 3 inches above the clamp on the edge of the front and tension faces disoriented the grain for about one-half the width of the tension face. Post impact strength: weakest of the RO 68 series.

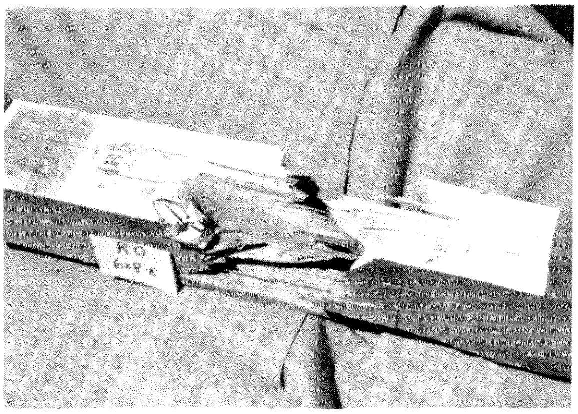

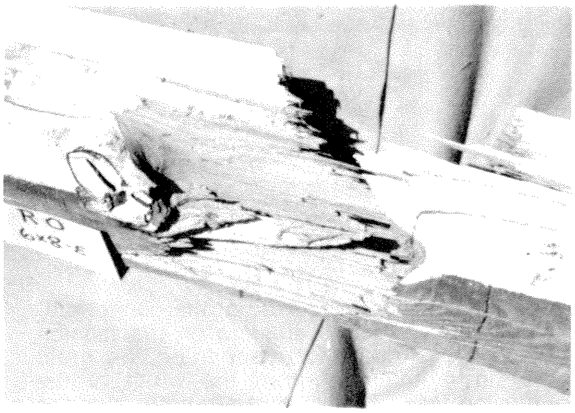

Table 1.—Red oak post pendulum-impact values to the point of major failure

Post No.	Area of post cross-section	Aver.[a] rings/inch	Specific[a] gravity	Moisture content at test	Pendulum velocity		Elapsed[c] time	Impulse	Fracture energy	Aver. force	Displacement	Peak force
					Impact	Final						
	Sq. in.	*No.*	*ODW/ODV*[b]	*Pct.*	*Ft./sec.*	*Ft./sec.*	*Msec*	*lb-sec*	*Ft-Kips*	*Kips*	*In.*	*Kips*
RO 66E	36.0	12	0.69	48	29.0	26.9	20	269	7.36	13.1	6.7	18.2
RO 66A	34.0	14	.74	73	25.0	23.2	19	230	5.53	12.1	5.5	19.5
RO 66B	36.6	7	.74	46	26.3	24.7	18	191	4.87	10.6	5.5	18.0
RO 66C	36.6	8	.67	52	25.4	23.9	18	184	4.53	9.2	5.9	15.5
RO 66DD	38.4	8	.73	41	25.7	24.3	18	174	4.34	9.7	5.4	16.7
Average	36.3	—	0.71	52	26.3	24.6	19	210	5.33	11.0	5.8	17.6
RO 68C	48.6	8	0.65	48	26.1	23.5	19	314	7.81	16.5	5.7	26.3
RO 68G	50.8	7	.64	57	26.0	23.6	20	302	7.48	15.1	6.0	24.0
RO 68B	52.9	7	.72	51	25.5	23.1	19	307	7.45	16.2	5.5	27.5
RO 68D	48.6	12	.66	57	26.4	24.3	19	271	6.86	14.3	5.8	24.5
RO 68A	51.5	6	.67	54	26.3	24.5	17	231	5.86	13.6	5.2	22.3
RO 68E	48.0	6	.63	73	25.7	24.0	16	221	5.49	13.8	4.9	20.7
Average	50.1	—	0.66	57	26.0	23.8	18	274	6.82	14.9	5.5	24.2

[a] Values determined from sample taken along a representative radius starting 1 inch from the pith.
[b] Oven-dry weight/oven-dry volume.
[c] 3 msecs subtracted from total time as shown on force-time curves to allow for compression of attenuation pad.

Figure 8.—Examples of force-time curves for red oak 6x6-inch and 6x8-inch posts (1 msec = 0.001 second). Shaded area is the impulse to major failure.

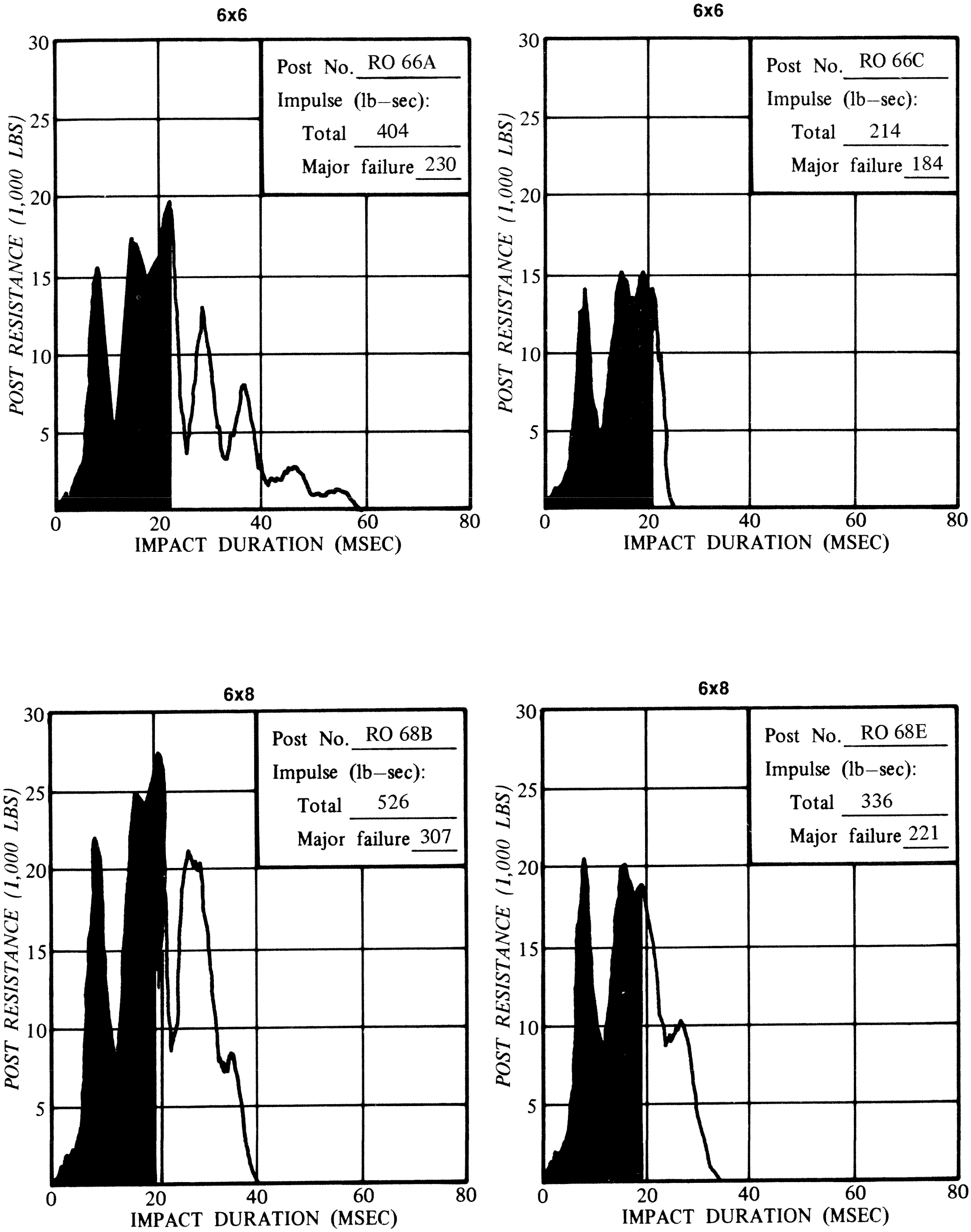

important defect affecting their performance as guardrail support. The specific location of knots within the post and the extent to which the grain is distorted around knots located at or near the point of greatest tensile stress can have a serious effect on strength. The effect of knots on compressive and shear strength is small.

Examples of critical and non-critical knots are shown in figure 7. None of the non-critical knots distorted the grain for more than one-third the width of the tension face. Those knots causing a reduction in strength distorted the grain for one-half or more the width of the tension face.

Red Oak

The impact data for the red oak 6x6 and 6x8 series are given in table 1. In all cases, the peak force was reached at or immediately before the point of major failure. For both groups, the elapsed time to peak force was about 18 msecs after the attenuation pad on the post had been compressed (about 3 msecs). The average peak force for the 6x6 posts was 17.6 Kips (kilopounds) and for the 6x8 posts was 24.2 Kips.

Eight of the 11 oak posts suffered shear failure either above or below the top of the clamp. There was no apparent relationship between impact values and whether or not there was shear failure. Also, whether the shear failure occurred above or below the clamp was unimportant. In the 6x6 group, for example, post RO 66E (the strongest) and post RO 66DD (the weakest) did not have shear failure. In the 6x8 group, RO 68C (the strongest) and RO 68A (second weakest) had shear failure above the clamp. Posts RO 68B, D, and G had shear failure below.

Examples of characteristic force-time curves for the red oak series are given in figure 8. Posts RO 66A and RO 68B had no strength-reducing defects. Each was about the strongest in its series. Post resistance increased until shear failure occurred. The unshaded area to the right of major failure represented the energy required to break the tension and compression sides following shear.

The force-time curves for RO 66C and RO 68E reflect the influence of strength-reducing knots. The reaction to impact of RO 66C was similar to that of RO 66A until 19 msecs had elapsed. At that point, RO 66C failed in tension at the clamp, and shear (major failure) above the clamp followed. The tension failure was affected by knot-associated grain distortion that covered more than one-third the width of the tension face. An additional knot cluster located 6 inches above the clamp on the front and compression faces caused the immediate failure of the compression side. After shearing, the compression side above the clamp can be viewed as a smaller post with knots on its tension face. Because of the knot cluster, there was no residual strength after the point of major failure.

The failure of RO 68E was affected by a 3-inch knot located about 3 inches above the clamp. The knot-associated grain distortion covered more than one-half the width of the tension and front faces. Failure started on the tension face and proceeded across the post's cross-section. Shear did not occur.

Southern Pine

The impact data for the southern pine series are given in table 2. In the untreated No. 1 SR series (SP 66, SP 86, and SP 68), failure was generally brashy to somewhat fibrous. Once begun, failure generally extended across the cross-section, without shear. The creosote-treated No. 1 Dense SR posts (SP 68_c) suffered more fibrous breaks, laminar failures at summerwood-springwood interfaces, and considerably less failure on the compression side. The greater resistance to impact of the treated posts was attributed mainly to the higher average percentage of summerwood per annual ring.

In the untreated series, strength values show the trends related to moments of inertia that were reported earlier (*Michie et al. 1971*). The SP 66 series was weakest of all. The SP 8x6 posts contained the same amount of wood as the SP 6x8 posts but were loaded about the minor axis. The SP 86 values fell between the SP 66 and SP 68 values.

Typical examples of force-time curves for the SP 66, SP 68, and SP 68_c (creosote-treated) series are given in figure 9. The southern pine curves are characteristically different from the red oak curves because of the

Table 2.—Southern pine pendulum-impact values to the point of major failure

Post No.	Area of post cross-section	Aver.[a] rings/inch	Percent[a] summer-wood	Specific[a] gravity	Moisture content at test	Pendulum velocity: Impact	Pendulum velocity: Final	Elapsed time[c]	Impulse	Fracture energy	Aver. force	Displace-ment	Peak force
	Sq. in.	*No.*	*Pct.*	*ODW/ODV*[b]	*Pct.*	*Ft./sec.*	*Ft./sec.*	*Msec*	*Lb-sec*	*Ft-Kips*	*Kips*	*In.*	*Kips*
SP 66C	35.4	5	28	0.58	22	26.1	24.8	18	168	4.27	9.3	5.5	14.5
SP 66F	35.4	5	30	.61	30	25.9	24.7	14	142	3.58	10.1	4.3	14.2
SP 66H	36.6	5	26	.49	23	26.3	25.3	16	127	3.27	7.9	5.0	13.7
SP 66D	35.4	8	31	.57	22	26.0	25.2	11	97	2.42	8.9	3.3	14.7
SP 66A	34.8	10	34	.59	22	26.7	26.0	10	91	2.39	9.1	3.2	13.7
SP 66B	36.0	5	17	.45	22	25.8	25.1	11	88	2.24	8.0	3.4	14.5
SP 66G	36.0	6	21	.45	20	25.7	25.1	9	69	1.76	7.7	2.8	12.5
Average	35.7	—	27	0.53	23	26.1	25.2	13	112	2.85	8.7	3.9	14.0
SP 86A	47.2	7	31	0.56	28	25.5	23.8	17	211	5.20	12.4	5.0	22.2
SP 86F	47.2	9	32	.55	20	28.9	27.4	15	175	4.93	11.7	5.1	19.7
SP 86C	47.8	9	33	.54	24	28.4	27.1	14	164	4.55	11.7	4.7	17.5
SP 86G	47.2	8	29	.55	22	28.7	27.5	14	146	4.12	10.4	4.7	16.5
SP 86B	48.0	7	28	.51	22	28.9	27.8	14	139	3.94	9.9	4.8	15.5
SP 86E	47.2	4	40	.56	28	29.2	28.4	11	105	3.04	9.6	3.8	16.5
SP 86D	48.0	4	21	.47	51	28.5	27.7	10	105	2.98	10.6	3.4	15.5
Average	47.5	—	31	0.53	28	28.3	27.1	14	149	4.11	10.9	4.5	17.6
SP 68F	48.0	7	29	0.61	23	28.4	26.1	20	278	7.58	13.9	6.5	24.0
SP 68A	46.6	8	35	.53	23	29.2	27.0	21	270	7.57	12.8	7.1	23.0
SP 68G	48.0	7	30	.52	29	27.1	25.1	21	250	6.51	11.9	6.6	19.8
SP 68B	47.2	6	43	.59	24	27.2	25.2	17	248	6.51	14.6	5.4	22.4
SP 68C	48.0	7	27	.50	25	28.8	26.9	18	225	6.26	12.5	6.0	20.9
SP 68E	48.6	5	24	.45	21	26.0	25.2	10	94	2.42	9.5	3.1	14.5
SP 68D	48.6	4	25	.49	21	28.3	27.6	11	89	2.50	8.1	3.7	14.5
Average	47.9	—	30	0.53	24	27.9	26.2	17	207	5.62	11.9	5.5	19.9
SP 68E$_c$	48.8	11	46	0.57	—	25.8	22.0	34	476	11.36	14.0	9.7	23.7
SP 68C$_c$	48.0	15	48	.60	—	25.8	23.4	27	431	10.39	16.0	7.8	24.5
SP 68G$_c$	47.4	4	44	.52	—	29.1	26.9	21	266	7.44	12.7	7.1	17.5
SP 68F$_c$	48.8	5	32	.46	—	26.4	24.3	20	263	6.68	13.2	6.1	18.7
SP 68A$_c$	48.2	7	39	.52	—	25.6	23.5	17	252	6.19	14.8	5.0	22.0
SP 68D$_c$	47.4	6	36	.49	—	26.3	24.3	19	238	6.03	12.5	5.8	16.9
SP 68B$_c$	47.4	7	36	.55	—	26.0	24.2	17	229	5.74	13.4	5.1	19.5
Average	48.0	—	40	0.53	—	26.4	24.1	22	308	7.69	13.8	6.7	20.4

[a] Values determined from sample taken along a representative radius starting 1 inch from the pith.
[b] Oven-dry weight/oven-dry volume.
[c] 3 msecs subtracted from total time as shown on force-time curves to allow for compression of attenuation pad.

Figure 9.—Examples of force-time curves for southern pine untreated No. 1 SR 6x6 and 6x8 posts and No. 1 dense creosote-treated 6x8 posts.

Untreated No. 1 SR southern pine 6x6-inch posts.

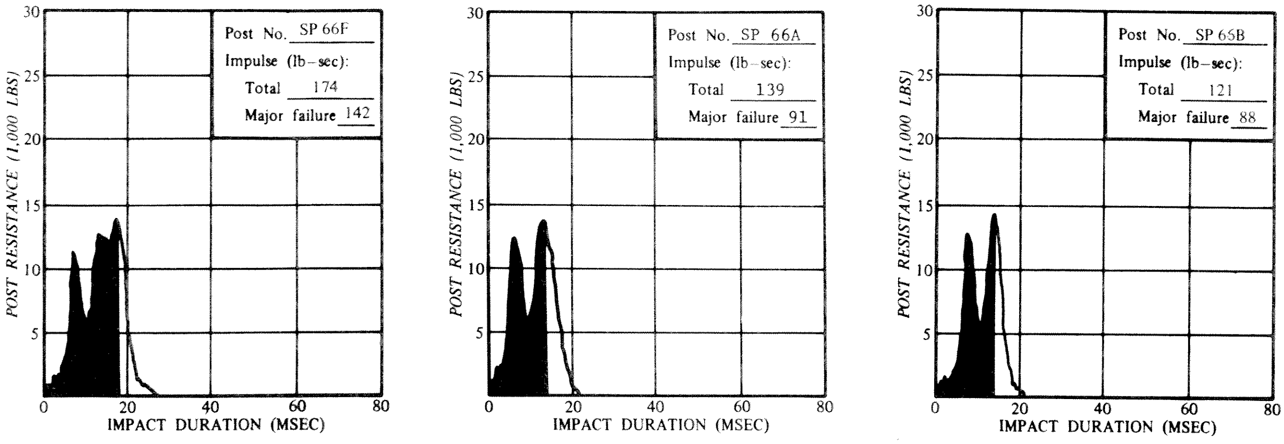

Untreated No. 1 SR southern pine 6x8-inch posts.

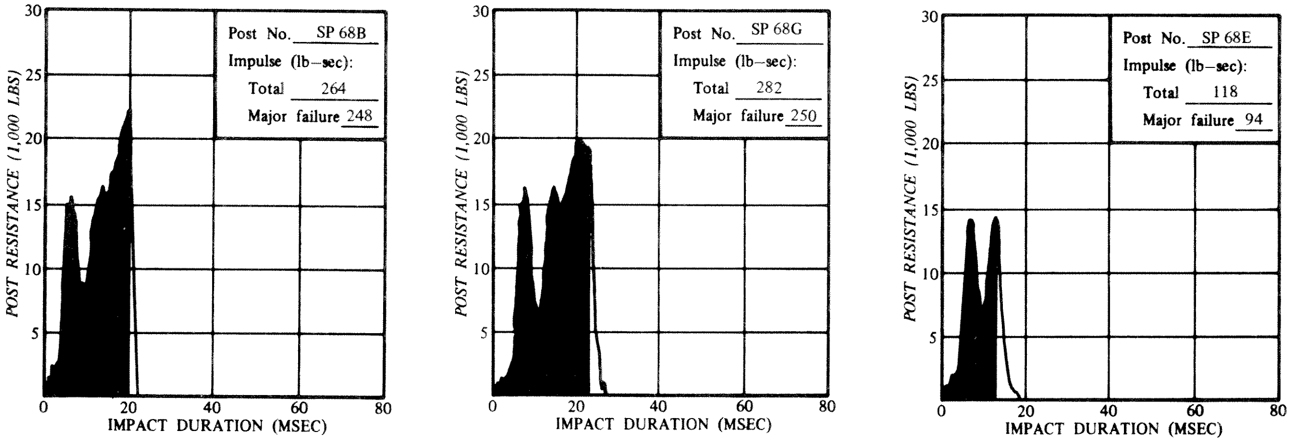

Creosote-treated No. 1 dense SR southern pine 6x8-inch posts.

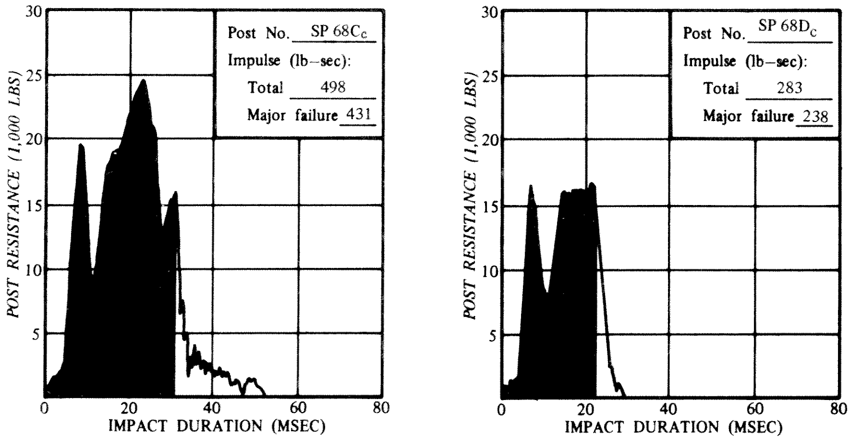

general absence of shear failure in the southern pine posts. Once major failure occurred across the cross-section, there was nothing left to offer resistance to the pendulum.

The SP 66F curve was typical of the stronger posts in the 66 series. For these posts (SP 66 C, F and H), there were no knots on the tension face in the middle third of the post, and failure was somewhat fibrous.

The influence of knot-associated grain distortion on strength is shown by a comparison of the curves of SP 66A and B. SP 66B had no knots influencing its failure. The low resistance to impact was attributed to the low percentage of summerwood (17 percent) and low specific gravity (0.45). SP 66A, with twice as much summerwood (34 percent) and a 25-percent greater specific gravity (0.59), performed in all respects the same as SP 66B. In the middle third of the tension face of SP 66A, there was a large knot that disoriented the grain for more than one-third the width of the face.

The influence of the amount of knot-associated grain distortion was most dramatically shown in the untreated SP 68 series. The force-time curve for SP 68G was about identical to that for the other strong posts in the series (SP 68A, B, C, and F), which had no knots in the middle third of the posts. SP 68G was average in percentage of summerwood and specific gravity. It had three knots located 4 to 6 inches above the clamp on the tension face (fig. 7). Though the total area covered by the knots was about three-fourths the width of the tension face, no single knot distorted the grain for more than one-third the width of the face. The main line of failure was in clear wood across the cross-section at the top of the clamp.

Posts 68E and D, though slightly low in percentage of summerwood and specific gravity, performed poorly because of knot-associated grain distortion. SP 68E (fig. 7) had a 1½-inch knot about 11 inches above the clamp that disoriented the grain across the entire 6-inch width of the tension face. Failure beginning immediately below this knot was clearly visible in the high-speed motion pictures. Other knots from the same cluster on the other faces had no effect.

Post SP 68D had the opposite knot configuration. Two 2-inch knots in the center and right edge of the tension face disoriented the grain for about one-half the width of the tension face. Failure of SP 68D, which began on the tension face, was unaffected by a single knot on the compression face that disoriented the grain for the entire 6-inch face width.

In the creosote-treated series (SP 68_c), SP $68D_c$ was the only post affected by knot-associated grain distortion. A 1-inch knot located 10 inches above the clamp distorted the grain for about one-half the width of the tension face. Failure began immediately below the knot.

SP $68C_c$ exhibited superior properties. Part of this excellent performance was attributed to high percentage of summerwood (almost 50 percent) and specific gravity (0.60). The manner of failure was also a factor. About the time that the peak resistance occurred, laminar failures occurred, beginning just below the tension face and moving toward the center of the post. These successive failures at the summerwood-springwood interfaces resulted in an extension of time to the point of major failure and increased the total resistance to impact.

Steel Posts

Data for the weak (S3x5.7) and strong (W6x8.5) steel posts are given in table 3 and figure 10. The post holder was modified for these posts to insure structural failure above the clamp. The slope on the front face of the T-brace was filled with a wooden block and a U-shaped metal insert was substituted for the pad at the top of the T.

With both types of steel posts, the peak force was reached at the beginning of the impact period rather than at the point of major failure as with wood. For the steel posts, the point of major failure was the point at which the post buckled. Failures occurred at or immediately above the clamp top. After the initial buckling, the energy bent the posts against the top of the clamp.

Even though the post holder was modified to prevent twisting, three of the seven S3x5.7 posts twisted after the point of major failure (posts C, E, and G). Three of the five W6x8.5 steel posts (D, E, and G) twisted at about the time of major failure.

Figure 10.—Examples of force-time time curves for S3x5.7 and W6x8.5 steel posts (1 msec = 0.001 second). Shaded area is the impulse to point of buckling.

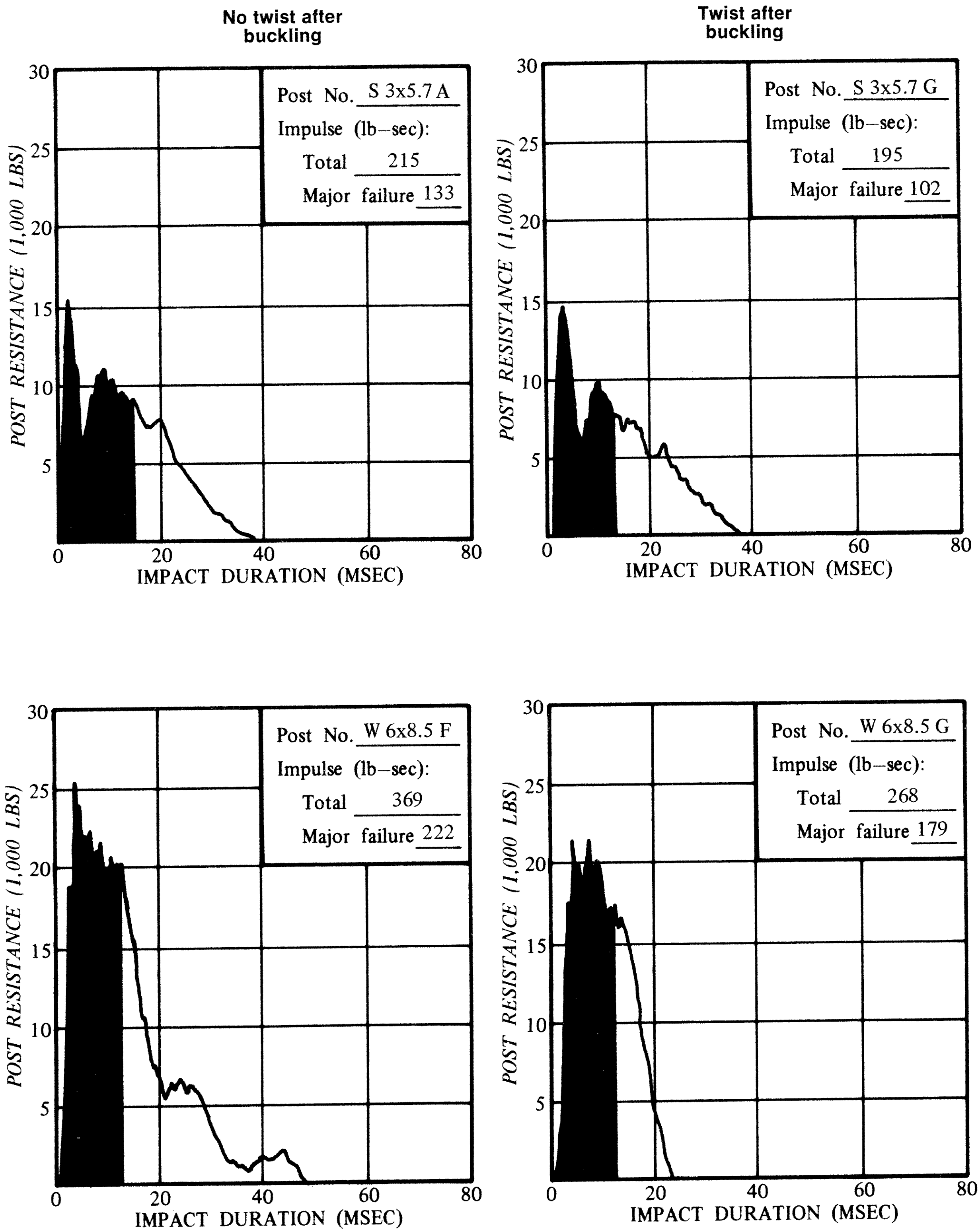

Table 3.—Steel-post pendulum-impact values to the point of major failure

Post No.	Pendulum velocity Impact	Pendulum velocity Final	Elapsed time	Impulse	Fracture energy	Aver. force	Displacement	Peak force
	Ft./sec.	*Ft./sec.*	*Msec.*	*Lb-sec.*	*Ft-Kips*	*Kips*	*In.*	*Kips*
S3x5.7A	30.2	29.1	15	133	3.95	8.9	5.3	15.5
S3x5.7F	29.7	28.8	13	107	3.13	8.2	4.6	15.1
S3x5.7G	26.6	25.8	13	102	2.66	7.8	4.1	14.9
S3x5.7B	26.2	25.4	13	102	2.63	7.8	4.0	13.2
S3x5.7E	26.1	25.3	14	102	2.61	7.3	4.3	14.5
S3x5.7D	26.0	25.2	13	98	2.51	7.5	4.0	16.0
S3x5.7C	26.0	25.4	9	68	1.78	7.7	2.8	13.1
Average	27.3	26.4	13	102	2.75	7.9	4.2	14.6
W6x8.5E	29.4	27.4	14	246	6.98	17.6	4.8	28.0
W6x8.5D	30.5	28.6	13	233	6.91	18.0	4.6	24.5
W6x8.5F	27.0	25.2	12	222	5.81	18.5	3.8	25.5
W6x8.5C	26.8	25.1	10	211	5.48	21.1	3.1	28.5
W6x8.5G	26.0	24.6	12	179	4.53	14.9	3.7	21.5
Average	27.9	26.2	12	218	5.94	18.0	4.0	25.6

The S3x5.7 posts are generally considered suitable for weak-post guarding systems, while the W6x8.5 posts are used in the strongpost systems. Both types had about the same average elapsed time to major failure (12 to 13 msecs) and displacement to major failure (about 4 inches). The other S3x5.7 parameters of fracture energy, average force, and peak force were about half those of the W6x8.5 steel posts.

DISCUSSION OF RESULTS

This report can be considered somewhat biased against wood. First, in each wooden-post series, posts with strength-reducing defects were purposely included. Second, in the steel-post series, force was applied only perpendicular to the flanges and parallel to the web (the strong axis). By modifying the post holder, efforts were made to prevent steel posts from twisting. The resulting values were used as indicators of overall steel-post performance even though impact against the weak axis (perpendicular to the web) would almost certainly reduce strength performance of steel posts in actual use.

In general, the better strong post is one that provides a lower peak resistance force and a lower average resistance force while at the same time maintaining an adequate fracture energy. Peak and average forces relate to the "G" forces acting on vehicle occupants. Fracture energy relates to the ability of a guardrail system to absorb the energy of impact. The average force is determined by dividing the fracture energy by the post displacement. The more resilient posts will provide greater displacements and, as a result, lower average force values.

Considering these factors, we found that wooden posts have characteristics that are equal or superior to those of comparable steel posts. The No. 1 SR 6x6 southern pine posts were directly comparable to the S3x5.7 steel posts. The red oak 6x6 posts (fig. 11) and the southern pine 6x8 No. 1 SR posts were, overall, slightly superior to the W6x8.5 steel posts. The red oak 6x8 posts and the No. 1 Dense SR creosote-treated southern pine posts were considerably superior to the W6x8.5 steel posts (fig. 12).

In making these comparisons, we considered fracture energy first. If the guarding system will not absorb the kinetic energy of vehicle impact, then other post properties are unimportant. If the W6x8.5 steel post is selected as the standard for comparison, then for strong-posts systems the fracture energy of the red oak 6x6 posts (5.33 ft-kips) and southern

Figure 11.—Examples of wooden posts after impact testing.

Figure 12.—Examples of steel posts after impact testing.

pine No. 1 SR 6x8 posts (5.62 ft-kips) were comparable to the W6x8.5 steel posts (5.94 ft-kips).

The wooden posts were more resilient and showed greater displacements to the point of major failure. Thus the average force values for the red oak and southern pine strong posts were two-thirds those for steel. In addition, the peak forces for the strong wooden posts were only two-thirds those for steel.

An overview of all wooden posts clearly shows that the grade of wooden posts is not a true indicator of post performance in a guardrail system. More significant is the amount of grain distortion around knots in the middle third of the tension face. Knot-associated distortion over one-third or less the width of the tension face has no recognizable influence on impact strength characteristics. Knots in the middle third of the other faces or in the outer thirds of the post can be ignored. This finding suggests that states specifying 8x8-inch wooden posts that meet stress-grade requirements are overspecifying.

By eliminating from tables 1 and 2 those posts that were clearly weakened by knot-associated grain distortion, new comparisons of wooden and steel posts are possible (table 4). As the strength-reducing weak axis of the steel posts is not a factor in these values, red oak 6x6 and SP 6x8 posts can be compared very favorably with the W6x8.5 steel posts for strong-post guardrail systems.

CONCLUSIONS

1. The analysis of force-time curves and high-speed motion pictures, in combination with sample inspection, provides an excellent method for comparing the reaction to impact of various materials.
2. For strong-post guarding systems, red oak 6x6 posts and southern pine 6x8 posts provide impact-strength characteristics that are superior to those of W6x8.5 steel posts. Southern pine 6x6 posts are equal to the S3x5.7 steel posts for use in weak-post systems.
3. As a guardrail post is used in a dynamic situation, specifications for wooden guardrail posts based on grades or stress ratings can be eliminated. Wooden-guardrail-post specifications should be based on the amount of knot-associated grain distortion in the middle third of the length of the tension face. Such knot-associated grain distortion should not exceed one-third the width of the tension face.
4. Knots in the outer thirds of the length of wooden guardrail posts have no effect on impact strength and can be ignored.

REFERENCE

Michie, Jarvis D., Charles J. Gatchell, and Theodore J. Duke.
1971. DYNAMIC EVALUATION OF TIMBER POSTS FOR HIGHWAY GUARDRAILS. Highw. Res. Rep. 343: 19-33. Highw. Res. Board, Washington, D. C.

Table 4.—Average impact values for steel posts and wooden post unaffected by knot-associated grain distortion

Posts	Fracture energy	Average force	Displacement	Peak force
Wood:	*Ft-Kips*	*Kips*	*In.*	*Kips*
RO 66	5.53	11.4	5.8	18.1
RO 68	7.40	15.5	5.8	25.6
SP 66 (No. 1 SR)	3.16	8.8	4.3	14.3
SP 86 (No. 1 SR)	4.55	11.2	4.9	18.3
SP 68 (No. 1 SR)	6.86	13.1	6.3	22.0
SP 68c (No. 1 Dense SR)	7.97	14.0	6.8	21.0
Steel:				
S3x5.7	2.75	7.9	4.2	14.6
W6x8.5	5.94	18.0	4.0	25.6